

Interaction between non-Bragg band gaps in 1D metamaterial photonic crystals

Juan A. Monsoriu

Departamento de Física Aplicada, Universidad Politécnica de Valencia, 46022 Valencia, Spain

jmonsori@fis.upv.es

Ricardo A. Depine and María L. Martínez-Ricci

Grupo de Electromagnetismo Aplicado, Departamento de Física, Facultad de Ciencias Exactas y Naturales, Universidad de Buenos Aires, Ciudad Universitaria, Pabellón I, C1428EHA Buenos Aires, Argentina

Enrique Silvestre

Departamento de Óptica, Universidad de Valencia, 46100 Burjassot, Spain

Abstract: We consider periodic multilayers combining ordinary positive index materials and dispersive metamaterials with negative index in some frequency range. These structures can exhibit photonic band gaps which, in contrast with the usual Bragg gaps, are not based on interference mechanisms. We focus on effects produced by the interaction between non-Bragg gaps of different nature: a) the zero averaged refractive index, b) the zero permeability and c) the zero permittivity gaps. Our analysis highlights the role played by the unavoidable dispersive character of metamaterials. We show that the degree of overlap between these bands can be varied by a proper selection of the constructive parameters, a feature that introduces novel degrees of freedom for the design of photonic band gap structures. The numerical examples illustrate the evolution of the dispersion diagrams of a periodic multilayer with the filling fraction of the ordinary material constituent and show a range of filling fractions where propagation in the multilayer is forbidden for any propagation angle and polarization.

© 2006 Optical Society of America

OCIS codes: (160.4670) Optical materials; (230.4170) Multilayers; (350.4010) Microwaves;

References and links

1. Y. Fink, J. Winn, S. Fan, C. Chen, J. Michel, J. Joannopoulos, and E. Thomas, "A Dielectric Omnidirectional Reflector," *Science* **282**, 1679-1682 (1998).
2. P. St. J. Russell, S. Tredwell, and P. J. Roberts, "Full photonic bandgaps and spontaneous emission control in 1D multilayer dielectric structures," *Opt. Commun.* **160**, 66-71 (1999).
3. D. N. Chigrin, A. V. Lavrinenko, D. A. Yarotsky, and S. V. Gaponenko, "Observation of total omnidirectional reflection from one-dimensional dielectric lattice," *Appl. Phys. A* **68**, 25-28 (1999).
4. C. Xudong, C. Hafner, R. Vahldieck, and F. Robin, "Sharp trench waveguide bends in dual mode operation with ultra-small photonic crystals for suppressing radiation," *Opt. Express* **14**, 4351-4356 (2006).
5. D. Delbeke, R. Bockstaele, P. Bienstman, R. Baets, and H. Benisty, "High-efficiency semiconductor resonant-cavity light-emitting diodes: a review," *IEEE J. Sel. Top. Quantum Electron.* **8**, 189-206 (2002).
6. Y. Akahane, T. Asano, B.-S. Song, and S. Noda, "High-Q photonic nanocavity in a two-dimensional photonic crystal," *Nature* **425**, 944-947 (2003).

7. J. Pendry (ed), Focus issue: Negative refraction and metamaterials, *Opt. Express* **11** (2003), <http://www.opticsexpress.org/ViewMedia.cfm?id=71852&seq=0>.
8. A. Lakhtakia and M. McCall (eds), Focus issue on negative refraction, *New J. Phys.* **7** (2005), <http://www.iop.org/EJ/abstract/-ff30=1/1367-2630/7/1/E03>.
9. D. Smith, J. Pendry, and M. Wiltshire, "Metamaterials and Negative Refractive Index," *Science* **305**, 788–792 (2004).
10. V. G. Veselago, "The electrodynamics of substances with simultaneously negative values of permittivity and permeability," *Sov. Phys. Usp.* **10**, 509–514 (1968).
11. J. Li, L. Zhou, C. T. Chan, and P. Sheng, "Photonic Band Gap from a Stack of Positive and Negative Index Materials," *Phys. Rev. Lett.* **90**, 083901 (2003).
12. L. Wu, S. He and L. Chen, "On unusual narrow transmission bands for a multi-layered periodic structure containing left-handed materials," *Opt. Express* **11**, 1283–1290 (2003).
13. H. Jiang, H. Chen, H. Li, Y. Zhang, J. Zi, and S. Zhu, "Properties of one-dimensional photonic crystals containing single-negative materials," *Phys. Rev. E* **69**, 066607 (2004).
14. L.-G. Wang, H. Chen, and S.-Y. Zhu, "Omnidirectional gap and defect mode of one-dimensional photonic crystals with single-negative materials," *Phys. Rev. B* **70**, 245102 (2004).
15. N. Panoiu, R. Osgood, S. Zhang, S. Brueck, "Zero-n bandgap in photonic crystal superlattices," *J. Opt. Soc. Am. B* **23**, 506–513 (2006).
16. L. I. Deych, D. Livdan, and A. A. Lisyansky, "Resonant tunneling of electromagnetic waves through polariton gaps," *Phys. Rev. E* **57**, 7254–7258 (1998).
17. R. A. Depine, M. L. Martínez-Ricci, J. A. Monsoriu, E. Silvestre, and P. Andrés, "Zero permeability and zero permittivity band gaps in 1D metamaterial photonic crystals," arXiv: physics/0606069 (2006).
18. I. Shadrivov, A. Sukhorukov, and Y. Kivshar, "Complete Band Gaps in One-Dimensional Left-Handed Periodic Structures," *Phys. Rev. Lett.* **95**, 193903 (2005).
19. P. Yeh, A. Yariv, and C. Hong, "Electromagnetic propagation in periodic stratified media. I. General theory," *J. Opt. Soc. Am.* **67**, 423–438 (1977).

1. Introduction

Photonic crystals (PCs) are periodic structures artificially designed to control and manipulate the interaction of light with matter. As a result of multiple interference of Bragg scattering, some frequencies are not allowed to propagate inside a PC, giving rise to forbidden and allowed bands, analogous to the electronic band gap of a semiconductor. The band structure depends on the PC's geometric and constitutive parameters, such as the lattice size or the contrast in refractive index. The interest in PCs microstructures has grown tremendously in the last decade because of the deep implications both from a fundamental and a technological point of view. In fact, spectacular new optical properties of PCs have been predicted, like lossless frequency selective mirrors [1, 2, 3], planar waveguides with sharp bends [4], high efficiency-surface light emitting diodes [5] or low-threshold lasers [6]. The recent fabrication of metamaterials [7, 8] has renewed interest in them. Metamaterials are artificially constructed composites exhibiting electromagnetic properties that are difficult or impossible to achieve with conventional, naturally occurring materials [9]. Key representatives of this new class of materials are metamaterials with negative index of refraction, a property that arises in media with a negative electric permittivity together with a negative magnetic permeability in the same frequency range [10]. Taking into account that the usual Bragg gaps are based on interference mechanisms, it follows that the middle frequency of the gap is inversely proportional to the lattice constant and therefore the size of real devices based on the photonic band gap is dependent on the working wavelength. Besides, interference mechanisms are affected by the inevitable presence of disorder, which may deteriorate the properties of the PC. In contrast, it has been shown that PCs made of metamaterials can also exhibit photonic band gaps which are not based on interference mechanisms [11, 12, 13, 14, 15], a fact that could enable the fabrication of devices based on PCs properties which are invariant to scale-length changes and robust against disorder.

In this paper we theoretically investigate the band structure of periodic bilayers containing metamaterials. We focus on the new effects produced by the interaction between two kinds of non-Bragg gaps that can coexist in PCs which combine ordinary materials and dispersive meta-

materials. The first kind of non-Bragg gap that we consider arises naturally when the volume averaged refractive index of the multilayer equals zero [11, 15]. Known as zero averaged refractive index, this gap can only be achieved in composites containing both conventional (positive index) materials and negative index metamaterials. At the frequency where the volume averaged refractive index vanishes, the periodic structure cannot support propagating modes and, unlike the Bragg gaps, the central frequency of this gap is invariant to the geometrical scaling of the superlattice. It is important to note that this invariance occurs provided that the constitutive parameters of the metamaterial are preserved, i.e., its internal structure is not scaled. The second kind of non-Bragg gaps that we consider appear as a direct consequence of the singular behavior near resonance of the effective permittivity and permeability of all available metamaterials. Previous studies on resonant tunneling of electromagnetic waves through polariton gaps [16] indicate that the singular behavior of the permittivity can give rise to peculiar frequency dependences of the tunneling penetration length, which results in tunneling properties that are qualitatively different from those of other optical barriers. It has been recently shown that the band structure of periodic multilayers containing dispersive metamaterials can exhibit non-Bragg gaps at frequencies where either the magnetic permeability μ or the electric permittivity ε of the metamaterial is zero [17]. Note that these gaps occur at frequencies where only a single constituent material of the multilayered structure intrinsically shows zero refractive-index, a situation that differs fundamentally from that of a multilayer whose unit cell combines two materials in such a way that the average of the refractive index is zero. As shown in [17], zero permeability and zero permittivity gaps are polarization dependent and therefore its existence cannot be ascribed to a breakdown of Snell's law when the refractive index is zero [14]. Additionally, the zero permeability and the zero permittivity gaps are also scale-length invariant and very robust against disorder. In this paper we study the band structure and the scattering properties of one-dimensional (1D) PCs which can exhibit both kinds of non-Bragg gaps, paying particular attention to new behaviors that can occur as a result of their interaction. We show that the degree of overlap between the zero averaged refractive index gap, the zero permeability and the zero permittivity gaps can be varied by a proper selection of constructive parameters, a feature that introduces novel degrees of freedom for the design of photonic band gap structures. We provide numerical examples that illustrate the evolution of the band structure of a periodic multilayer with the filling fraction of the ordinary material constituent, showing a range of filling fractions where propagation in the multilayer is forbidden for any propagation angle and polarization [18]. Our analysis highlights the important role played by the unavoidable (and usually strong) dispersive character of metamaterials, a point that usually plays a secondary role, or is even neglected in the design of photonic band gap structures.

This paper is organized as follows: Section 2 is devoted to summarize the main properties of non Bragg gaps, Section 3 is devoted to numerical results and concluding remarks are provided in Section 4. An $\exp(-i\omega t)$ time-dependence is implicit throughout the paper, with ω the angular frequency, t the time, and $i = \sqrt{-1}$.

2. Theory

We first consider the 1D periodic structure consisting of layers of two different materials: a conventional dielectric with permeability μ_1 , permittivity ε_1 and thicknesses d_1 , and a dispersive metamaterial with permeability $\mu_2(\omega)$, permittivity $\varepsilon_2(\omega)$ and thicknesses d_2 . The period of the structure is $d = d_1 + d_2$. The stratification direction is the y axis and we consider wave propagation in the $x - y$ plane. Let the function $f(x, y)$ represent the z -directed component of the electric field for the TE-polarization case (electric field parallel to the layers), and the z -directed component of the magnetic field for the TM-polarization case (magnetic field parallel to the layers). The propagating waves in the periodic structure have the form of Bloch modes,

for which the fields satisfy the condition $f(x, y + d) = f(0, y) \exp i(k_x x + Kd)$, where k_x is the wave vector component along the layers and K is the Bloch wave number. In order to obtain the dispersion relation we have used the transfer matrix formalism [19]. In it, the half trace of the transfer matrix characterizing the unit cell provides $K(\omega, k_x)$ through the following equation

$$\cos(Kd) = \cos(k_{1y}d_1) \cos(k_{2y}d_2) - \frac{1}{2} \left[\frac{\sigma_2 k_{1y}}{\sigma_1 k_{2y}} + \frac{\sigma_1 k_{2y}}{\sigma_2 k_{1y}} \right] \sin(k_{1y}d_1) \sin(k_{2y}d_2), \quad (1)$$

where the index $j = 1, 2$ indicates the layer, $\sigma_j = \mu_j$ for TE polarization or $\sigma_j = \varepsilon_j$ for TM polarization, $k_{jy}^2 = k_j^2 - k_x^2$, and $k_j = \omega n_j / c$ are wave numbers in each media with refractive indexes n_j .

The usual Bragg forbidden bands (or gaps) of the periodic medium occur under the following conditions [12]

$$k_{1y}d_1 + k_{2y}d_2 = p\pi, \quad p = \pm 1, \pm 2, \dots, \quad (2)$$

$$\sigma_2 k_{1y} \neq \sigma_1 k_{2y} \quad (3)$$

$$k_{1y}d_1 \neq q\pi, \quad q = 1, 2, \dots \quad (4)$$

In this case, the absolute value of the right hand side of Eq. (1) is greater than unity, K has an imaginary part and the Bloch wave is evanescent. Unusual transmission bands, reported in Ref. [11], occur when only the conditions (2) and (3), but not condition (4), hold.

Metamaterial multilayers can also exhibit non-Bragg gaps. We focus on the interaction between: a) the $\bar{n} = 0$ gap (\bar{n} being the average refractive index of the unit cell) and b) the zero permeability and zero permittivity gaps [17]. The $\bar{n} = 0$ gap occurs when the conditions

$$\left. \begin{array}{l} \sigma_2 k_{1y} \neq \sigma_1 k_{2y} \\ k_{1y}d_1 + k_{2y}d_2 = 0 \end{array} \right\} \quad (5)$$

are simultaneously attained, which is impossible if both layers in the unit cell have either positive or negative refractive index. The middle frequency of this gap does not depend on the period d . The zero permeability and zero permittivity gaps occur at frequencies where a constitutive parameter of the metamaterial –either $\mu_2(\omega)$ or $\varepsilon_2(\omega)$ – changes its sign. Contrary to the $\bar{n} = 0$ gap, the zero permeability and zero permittivity gaps occur at frequencies where only a single constituent material of the multilayered structure intrinsically shows zero refractive-index. Note that the term between square brackets in the right hand side of Eq. (1) becomes singular under these conditions, except for propagation along the stratification direction ($k_x = 0$), where $k_{2y} \rightarrow 0$ and the singularity is compensated [17]. To be specific, let us assume that $k_x = 0$ and $\varepsilon_2 \rightarrow 0$ but $\mu_2 \neq 0$. In this limit, $k_{2y} \rightarrow 0$ and the dispersion relation (1) at normal incidence adopts the form

$$\cos(Kd) \approx \cos(k_1 d_1) - \frac{1}{2} \frac{\omega}{c} \sqrt{\frac{\varepsilon_1}{\mu_1}} \mu_2 d_2 \sin(k_1 d_1). \quad (6)$$

We observe that the right hand side in Eq. (6) can take any real value (just changing, for instance, the value of d_2), giving propagating Bloch modes when it belongs to the interval $[-1, 1]$ or evanescent Bloch modes when it is outside the interval $[-1, 1]$. A similar conclusion can be obtained when $\mu_2 \rightarrow 0$ but $\varepsilon_2 \neq 0$. For oblique incidences, on the other hand, $k_x \neq 0$, $k_{2y} \rightarrow \pm i k_x \neq 0$ and the second term in the right hand side of Eq. (1) remains singular when $\mu_2 = 0$

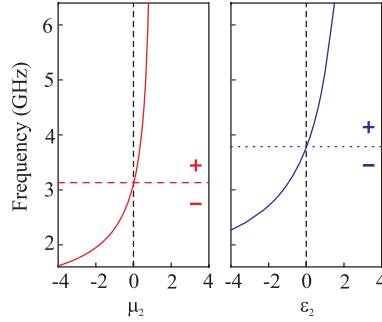


Fig. 1. Frequency dependence of the effective parameters μ_2 and ϵ_2 , as given by Eqs. (7). Note that μ_2 and ϵ_2 become zero at different frequency values, indicated by horizontal lines (3.133 and 3.787 GHz, respectively).

(TE polarization) or when $\epsilon_2 = 0$ (TM polarization), thus originating new gaps, not present for normal incidences. We conclude that the zero permeability and zero permittivity gaps always appear for oblique incidences: the $\mu_2 = 0$ gap appears for TE, but not for TM, polarization; whereas the $\epsilon_2 = 0$ gap appears for TM, but not for TE, polarization, i. e., it is a polarization dependent phenomenon. The greatest challenge in the field of photonic band gap structures has been the fabrication of composite structures possessing Bragg gaps at a given desired frequency. Up to now, this task has been mainly achieved by designing different lattices, periodicities, filling ratios or refractive index contrasts. Dispersion properties of the materials, on the other hand, have played a secondary role in the design of photonic band gap structures. In contrast, we see that dispersion properties play a key role in the appearance of the kind of non-Bragg gaps we have just discussed. This fact suggests that by tailoring dispersion properties of a metamaterial, we could obtain multilayers with very different band structures, a feature that introduces novel degrees of freedom for the design of photonic band gap structures.

3. Numerical results and discussion

For multilayers comprising both positive and negative index dispersive materials, the $\bar{n} = 0$ condition will always be met for some particular frequency. On the other hand, the zero permeability gap will appear at the particular frequency ω_μ where $\mu_2 = 0$, whereas the zero permittivity gap will appear at the particular frequency ω_ϵ where $\epsilon_2 = 0$. In previous studies on the appearance of non Bragg gaps in metamaterial multilayers, the $\bar{n} = 0$ gap and the zero permeability and zero permittivity gaps have been studied separately, without considering possible interaction between them. The purpose of this section is to illustrate this interaction through numerical results for a 1D system with alternate layers of air as a positive index material ($\epsilon_1 = \mu_1 = 1$) and dispersive metamaterial with a negative index in some frequency range. In the examples we assume that the effective constitutive parameters of the metamaterial are given by [11]

$$\begin{aligned}\epsilon_2(v) &= 1 + \frac{5^2}{0.9^2 - v^2} + \frac{10^2}{11.5^2 - v^2}, \\ \mu_2(v) &= 1 + \frac{3^2}{0.902^2 - v^2},\end{aligned}\tag{7}$$

where v is the frequency measured in GHz. The frequency dependence of the effective parameters μ_2 and ϵ_2 is shown in Fig. 1. Note that μ_2 and ϵ_2 become zero at different frequency values, indicated by red dashed ($\omega_\mu/2\pi = 3.133$ GHz) and blue dotted ($\omega_\epsilon/2\pi = 3.787$ GHz)

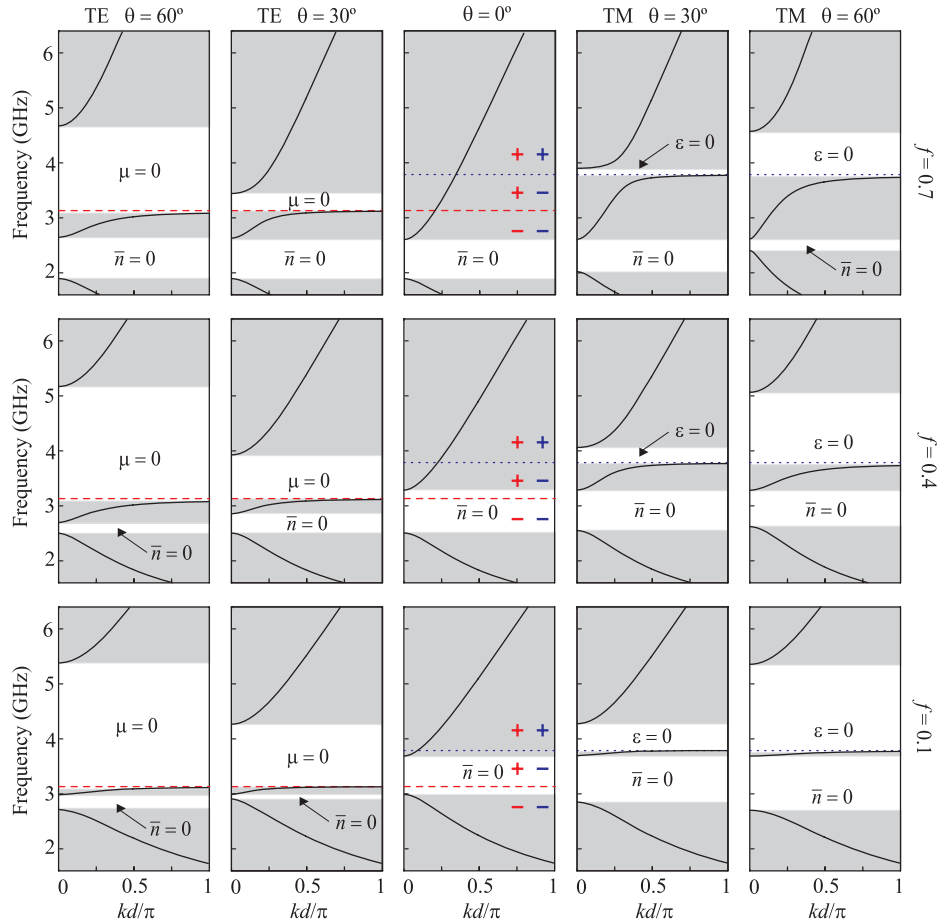


Fig. 2. Band structure for TE and TM polarizations, different angles of incidence and different filling fractions (f) corresponding to periodic stacks (period $d = 15$ mm) with air layers ($\mu_1 = \epsilon_1 = 1$, $d_1 = fd$) and MM layers (μ_2 and ϵ_2 shown in Fig. 1, $d_2 = (1 - f)d$). Note that the zero permeability and the zero permittivity gaps are absent for normal incidence (central column).

lines respectively. We fix the period of this structure to $d = 15$ mm. The widths of the air and metamaterial layers are $d_1 = fd$ and $d_2 = (1 - f)d$, where f is the air filling fraction.

The evolution of the band structure with angle of incidence, polarization and air filling fraction is shown in Fig. 2, for angles of incidence $\theta = 0^\circ$, 30° , 60° and three different values of the air filling fraction: $f = 0.1$ (bottom row), $f = 0.4$ (central row) and $f = 0.7$ (top row). Beginning with the central column, corresponding to the band structure at normal incidence ($k_x = 0$), only a non Bragg gap, corresponding to the condition $\bar{n} = 0$, occurs in the considered frequency range. When the air filling fraction is decreased from $f = 0.7$ (top row) to $f = 0.1$ (bottom row), the central frequency of the $\bar{n} = 0$ gap moves up, because less negative values of the metamaterial refractive index are required to satisfy the $\bar{n} = 0$ condition (as seen in Fig. 1, in the frequency range considered, the less negative values of the metamaterial refractive index occur at higher frequencies).

We observe that in the $f \rightarrow 0$ limit (an homogeneous metamaterial) the $\bar{n} = 0$ gap at normal incidence tends to coincide with the region delimited by ω_μ and ω_ϵ (indicated by red dashed and

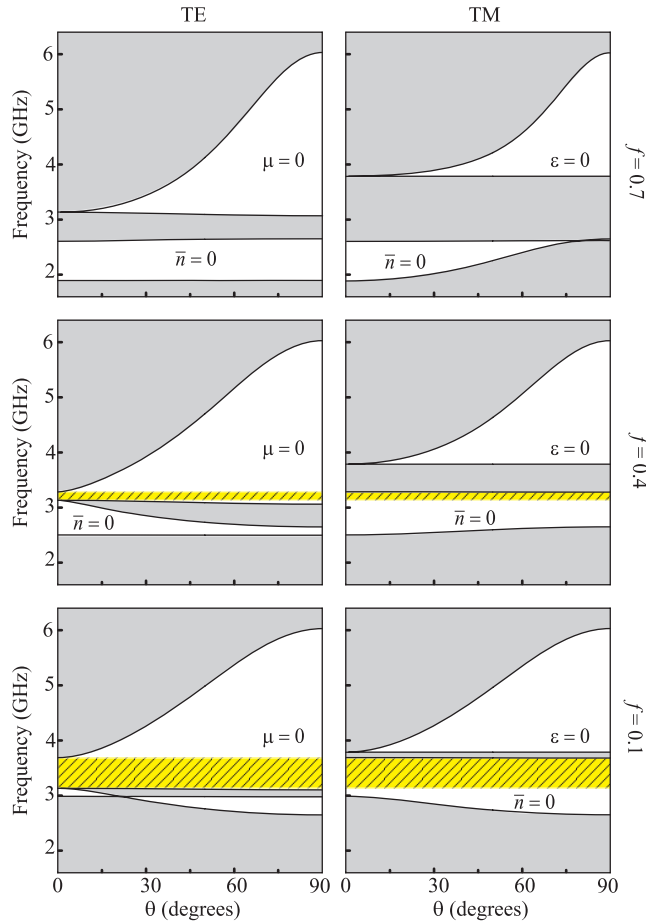


Fig. 3. Projected band structure for TE and TM polarizations corresponding to the periodic stacks considered in Fig. 2.

blue dotted lines in Fig. 2), where the metamaterial behaves as an optical insulator ($\epsilon_2 \mu_2 < 0$). Note that frequency regions near ω_μ (where $\mu_2 = 0$) and ω_ϵ (where $\epsilon_2 = 0$) may correspond to allowed states, despite the fact that in these regions the metamaterial exhibits zero refractive index (see, for example, the band diagram corresponding to $f = 0.7$).

The central column in Fig. 2 shows that the overall effect of varying the air filling fraction is to tune the $\bar{n} = 0$ gap in order to include or exclude frequency regions where constitutive parameters of the metamaterial become zero. For normal incidence, this tuning effect does not seem to change the band diagrams since, as predicted by Eq. (6), the otherwise forbidden states corresponding to zero permeability and zero permittivity, are now allowed. However, for oblique incidences, this tuning effect changes substantially the band diagrams. New gaps appear near regions where a constitutive parameter changes its sign. This is shown in side columns in Fig. 2, corresponding to TE and TM polarizations and oblique incidences ($\theta = 30^\circ$ and 60°). A relevant feature shown by these band diagrams is that, although the refractive index vanishes at frequencies where the constitutive parameters are zero, the new gap associated to $\mu_2 = 0$ appears only for TE, but not for TM, polarization; whereas when $\epsilon_2 = 0$ the new gap appears for TM, but not for TE, polarization.

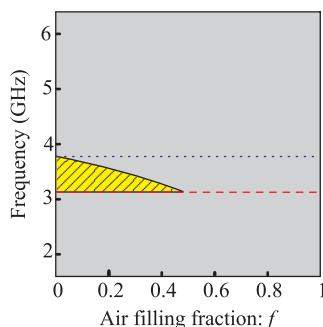


Fig. 4. Dependency of the region of omnidirectional reflection on the air filling fraction f .

As a consequence of the appearance of these new gaps at oblique incidences, new conduction bands appear between the $\bar{n} = 0$ gap and the $\mu_2 = 0$ gap (TE polarization) and between the $\bar{n} = 0$ gap and the $\varepsilon_2 = 0$ gap (TM polarization). For low values of the air filling fraction, the width of the new conduction band (see last row in Fig. 2 corresponding to $f = 0.1$) is extremely narrow. The low curvature of the dispersion relation will imply a high density of states in this frequency range.

The projected band structure for TE and TM polarizations, corresponding to the periodic stacks considered in Fig. 2, is shown in Fig. 3. White regions indicate bands where propagation is forbidden, regardless of K . For $f = 0.7$, the $\bar{n} = 0$ gap provides omnidirectional reflection for TE polarization but not for TM polarization, whereas the $\mu_2 = 0$ gap for TE polarization and the $\varepsilon_2 = 0$ gap for TM polarization do not strictly correspond to omnidirectional reflection because, as discussed above [see Eq. (6)], zero permeability and zero permittivity gaps do not necessarily occur at normal incidence and they are absent for this value of the air filling fraction. Note that in this example, no interaction occurs between non Bragg gaps of different origin and no frequency interval leading to omnidirectional reflection for both TE and TM polarizations can ever be found. However, by decreasing the value of the air filling fraction, the $\bar{n} = 0$ gap approaches to frequency regions where a constitutive parameter vanishes. In our case, since $\omega_\mu < \omega_\varepsilon$, the $\bar{n} = 0$ gap interacts firstly and more strongly with the $\mu_2 = 0$ gap for TE polarization. As a consequence of this interaction, the $\bar{n} = 0$ gap for this polarization becomes narrower while the $\mu_2 = 0$ gap widens accordingly.

In this way, we notice that, at normal incidence and for low air filling fractions, the band gap labeled as $\bar{n} = 0$ gap in Fig. 2, should have been considered as a juxtaposition of $\bar{n} = 0$ and $\mu_2 = 0$ gaps, as evidenced by the field characteristics at both sides of the gap.

As a consequence of the intersection of these bands, a forbidden region for all angles of incidence (including normal incidence) and polarizations appears. In these regions, indicated by yellow striped zones in Fig. 3, the multilayer behaves as a perfect reflector for both polarizations and all angles of incidence.

For the parameters corresponding to Fig. 3, the dependency of the region of omnidirectional reflection on the air filling fraction f is shown in Fig. 4. For $f = 0$ we do not have a multilayer but a metamaterial that behaves like a metal, providing full reflection in the range $\omega_\mu < \omega < \omega_\varepsilon$ (the region between red dashed and blue dotted lines in Fig. 4). As f increases, the upper limit of this region (coinciding with the upper limit of the $\bar{n} = 0$ gap for TM polarization) decreases, whereas the lower limit of the gap remains near ω_μ . The region of omnidirectional reflection disappears when $f \geq 0.485$, since at these values of air filling fractions, ω_μ falls outside the $\bar{n} = 0$ gap.

To illustrate the properties of finite structures, we show in Fig. 5 the TE and TM reflectivity

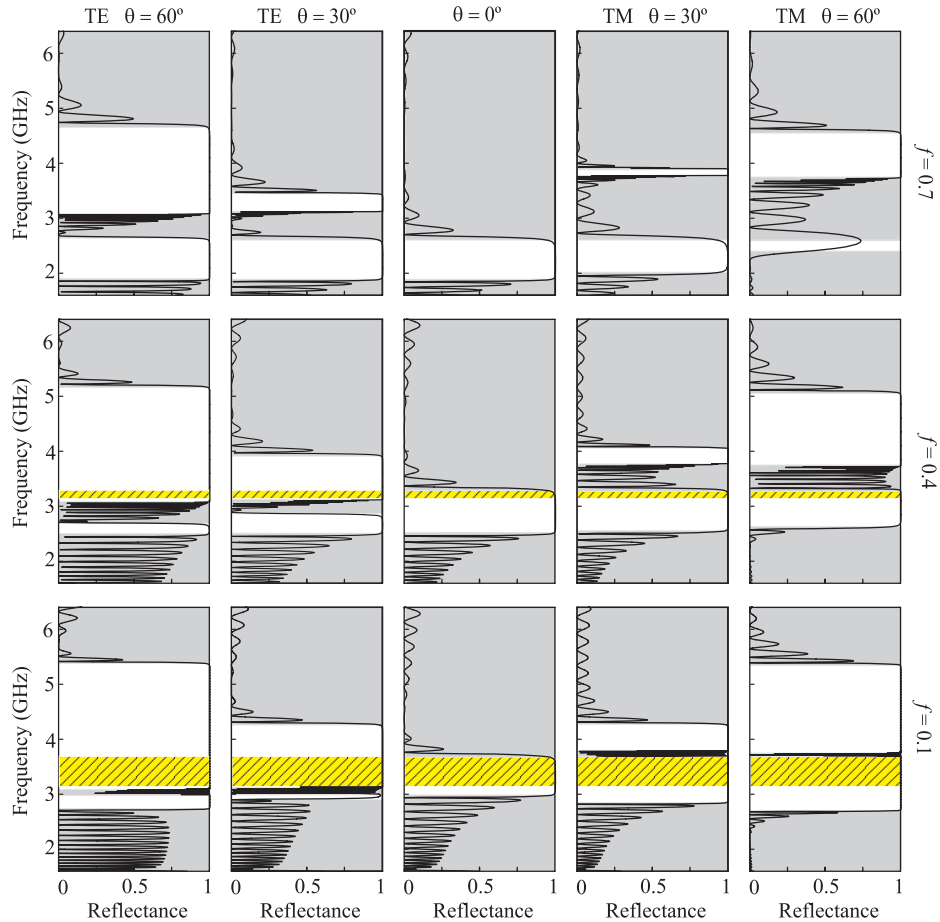


Fig. 5. TE and TM reflectivity through 16 unit cells corresponding to the band structures in Fig. 2.

through 16 unit cells corresponding to the band structures presented in Fig. 2. Grey regions correspond to conduction bands, with very low reflectivity values, whereas white regions correspond to forbidden bands with reflectivity ≈ 1 . On top of the white regions we mark with yellow stripes the frequency range corresponding to omnidirectional reflection. We can observe that the locally periodic finite system maintains the main characteristics observed above for the perfectly periodic infinite system.

4. Conclusion

We have studied the interaction between two kinds of photonic band gaps which, in contrast with the usual Bragg gaps, are not based on interference mechanisms. Our analysis highlights the important role played by the unavoidable (and usually strong) dispersive character of metamaterials, a point that usually plays a secondary role, or is even neglected in the design of PCs made of ordinary materials. We have shown that the degree of overlap between the zero averaged refractive index gap, the zero permeability and the zero permittivity gaps can be varied by a proper selection of constructive parameters, a feature that introduces novel degrees of freedom for the design of photonic band gap structures. We have presented numerical examples

that illustrate the evolution of the dispersion diagrams with the filling fraction of the ordinary material constituent, showing a range of filling fractions where propagation in the multilayer is forbidden for any propagation angle and polarization.

This work was funded by the Plan Nacional I+D+i (grant TEC2005-07336-C02-02/MIC), Ministerio de Educación y Ciencia, Spain, and FEDER. RAD acknowledges financial assistance provided by the Universidad de Valencia (Programa de Estancias Temporales para Investigadores Invitados). MLMR acknowledges partial support from Consejo Nacional de Investigaciones Científicas y Técnicas (CONICET), Universidad de Buenos Aires (UBA) and Agencia Nacional de Promoción Científica y Tecnológica (ANPCYT-BID 802/OC-AR03-14099). J.A.M. also acknowledges financial support from the Plan Nacional I+D+i (grant FIS2005-01189).